Asociación Argentina
de Mecánica Computacional

Mecánica Computacional Vol XXXVIII, págs. 457-467 (artículo completo)
H.G. Castro, J.L. Mroginski, R.R. Paz, M.A. Storti (Eds.)
Resistencia, 1-5 Noviembre 2021

COMPUTATIONAL FLUID DYNAMICS AS AN ENGINEERING TOOL FOR LAMINAR FLOW ELEMENT MASS FLOW CONTROLLER DESIGN

G. Imbrioscia[a,d], A. Larreteguy[b], P. Pantaleo Demaldé[c] and M.J. Lavorante[a]

[a]*Division de Investigación y Desarrollo en Energías Renovables (DIDER), Instituto de Investigaciones Científicas y Técnicas para la Defensa (CITEDEF), San Juan Bautista De La Salle 4397,B1603ALO,Villa Martelli, Bs.As., Argentina, gimbrioscia@citedef.gob.ar*

[b]*Instituto de Tecnología, Universidad Argentina de la Empresa (UADE), Lima 775, C1073AAO Ciudad Autónoma de Buenos Aires, Argentina,alarreteguy@uade.edu.ar*

[c]*INGENES soluciones con ingenieria, Bs.As.,info@ingenes.com.ar, https://www.ingenes.com.ar/*

[d]*Grupo de Investigacion en la Mecánica de la Fractura (GIMF), Universidad Tecnológica Nacional Regional Haedo (UTN-FRH), París 532,B1706EAH, Haedo, Bs.As., Argentina*

Keywords: OpenFOAM, LFE, Poiseuille flow, mass flow controller.

Abstract. In order to provide an accurate gas flow rate value to a Polymer Electrolyte Membrane Fuel Cell, a Poiseuille Gas Flowmeter (PGF) was designed and validated through Computational Fluid Dynamics (CFD) simulations. The device is based on the inclusion of a Laminar Flow Element (LFE), aimed at forcing the incoming flow into a laminar flow by using different geometric arrangements, like calibrated small diameter pipes or thin parallel planar ducts. Once laminar flow is achieved, the Poiseuille equation for the corresponding shape can be used to calculate the mass flow rate based on differential pressure measurements. The open source CFD tool OpenFOAM® was used to adjust and validate different design parameters in order to obtain a feasible and cost effective device.

1 INTRODUCTION

Polymer Electrolyte Membrane Fuel Cell (PEMFC) uses oxygen and hydrogen to promote the water reaction in a controlled environment, transforming chemical energy into electricity and heat. This energy conversion system requires both precise gas delivery to control the stoichiometry of the reaction and specific gas humidity conditions to sustain the device useful life, thus turning the gas mass flow rate measurement process complex. The mass flow controller is therefore usually located between the pressure regulator and the humidifier, thus measuring dry streams.

Different technologies and techniques are used to measure mass flow rate of fluids, such as for example: *oval counter-synchronized rotors*, with gears interlocked to rotate with the flow; *propellers*, with paddles turning due to fluid impact; *magnetical*, in which coils produce a flow dependent magnetic field; *turbines*, with a bladed rotor axially aligned with the flow stream; *thermal dispersion*, where a sidestream flow of gas is directed through a heated capillary resulting in a flow dependent temperature gradient, and *differential pressure meters*, where the flow rate is related to a pressure change inside the device Baker (2016). From these options, the last three are recommended for dry gas streams. However, considering the gases involved in our process, differential pressure meters seem to be the safest option as there is nor heating devices neither rotating parts connected to inductors that could produce sparks. Furthermore, among the variety of differential pressure technologies, the laminar flow element approach is selected as it is present in many commercial devices.

This work presents a parametric study of a pressure differential LFE using Computational Fluid Dynamics (CFD), more specifically the open-source code OpenCFD (2017) ®, in a reverse engineering design process.

1.1 Design process

The device is based on the use of a Laminar Flow Element (LFE) Parmer (2021); Controls (2021); Meriam (2021a,b). This design concept searches for turning the incoming flow into laminar flow using different geometric arrangements as calibrated holes or parallel planar thin ducts.

In viscous flowmeters, pressure difference is measured in two selected positions separated by a precisely known distance. Two are two options: plenum pressure measurement or single channel measurement. The first option has the advantage of simpler port manufacturing but requires special calibration in order to compensate for drag and dynamic fluid behavior. Because of this, we decided to implement the second option.

A prototype with parallel planar thin ducts is considered in this work, as shown in figures 1a and 1b. The flow is received in an inlet plenum and forced to pass through the planar ducts towards the outlet plenum. The three parallel channels configuration was selected based on pressure sensor availability and flow management, as it will be discussed in the following sections.

In the single channel configuration the Poiseuille equation can be used to calculate flow rate based on the differential pressure measurements. In the present design, with parallel planar thin ducts, these reads

$$\Delta P = \frac{12 Q_c L_{dp} \mu}{h^3 w} \tag{1}$$

with Q_c volumetric flow rate, L_{dp} length between measuring ports, μ fluid dynamic viscosity, and h and w channel height and width, respectively. Pressure measurements will be performed

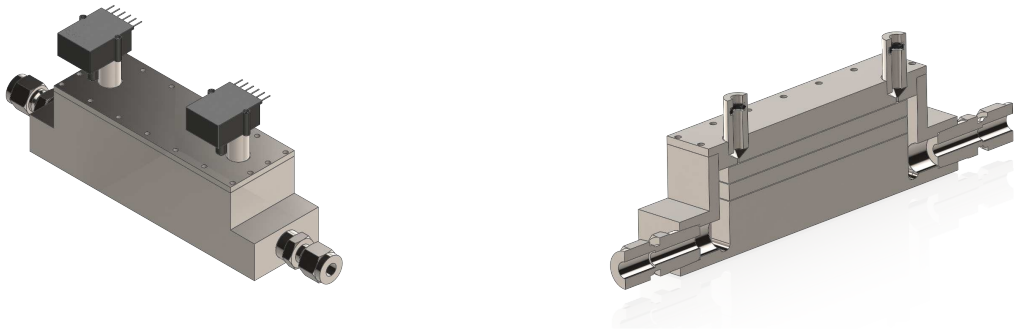

(a) Flow meter prototype (b) Flow meter prototype slice

Figure 1: Flow meter prototype proposed design

using Differential pressure sensors (Honeywell, 2021).

Laminar Flow Elements have two major drawbacks, because they require the gas to be either dry or with a minimum amount of humidity and the manufacturing process to work with a very high precision. The former responds to the possible partial blockage of the channels due to condensation, affecting the amount of gas that flows along each channel and hence the pressure difference, which is measured on only one of the channels. The latter is related to the strict tolerances of the final shape of the channel, where a variation of just 0.01 mm on the thickness severely affects the pressure measurement. This manufacturing limitation, plus the need to use materials adequate for hydrogen and oxygen environments, increases the cost of the device, thus making it important to have an optimized design.

1.1.1 Manufacturing process

In order to reduce the cost of production, two manufacturing process will be taken into account: conventional machining process and additive manufacturing technology.

Machining process: the material selected is stainless steel 316L because of its corrosion resistance properties. This selection, however, negatively influences the production time as it is non-magnetic, thus making the machining process more complicated due to the need of external jigs to keep the raw material in place instead of a magnetic vise, also affecting the precision of the finishing procedure. The major challenge in the design is the creation of the gap for the channel in a repeatable way. According to the design of commercial flowmeters, the gap may be produced by a separation plate, or *shim*, fitted between rectified gauges. This can also be achieved, however, by machining the channel itself. Due to manufacturing and budget limitations, the selected option was that of machining calibrated gauges and using stainless steel shims. For these shims, thin metal sheets are available in different thicknesses of 0.07, 0.1, 0.15 or 0.2 mm, providing options for the final configuration.

Additive manufacturing: between the available technologies, the selected ones should be capable of reaching the desired height of the channel. This reduces the choices down to two, namely Resin Based and Laser Sintering. Both can reach printing tolerances in the order 0.1 mm, making them promising options as design can be produced at once. However, surface finish, which can influence the channel behavior, is not under control.

If additive manufacturing is selected, the design should take into account overall thickness to ensure that the device will withstand the inner pressure. Also, chemical compatibility between

selected resins and measured fluids should be checked.

1.1.2 Pressure transducer

To avoid overshooting and reduce linearity error, it was decided that the pressure sensor for differential pressure measurements should operate at about half its operation range. Among the sensors considered, the Honeywell SCX1DN was the one that better satisfied the requirements among the locally available devices. It gives a voltage output which is directly proportional to the applied pressure. It is radiometric to the supply voltage and changes in the supply voltage will cause proportional changes in the offset voltage and full-scale span. The sensor operating range is 0-6895 Pa, which puts the operating pressure at about its half. It was calibrated for span to have a ± 1 error, so the maximum expected sensor error is ± 68.95 Pa or $\pm 49.51 \mathrm{mV}$, around 2% of the operating pressure. A supply voltage of 3.3 V was used, giving a sensitivity of 0.718 $\mathrm{mV/Pa}$ and a full scale span of $4.95 \mathrm{mV}$.

The analog to digital converter (ADC) used to acquire the sensor signal was the ADS1015. This features a 12-bit resolution, an internal low-drift voltage reference and a programmable gain amplifier. The error produced by the ADS1015 for the operating pressure is less than ± 125 $\mu\mathrm{V}$ or $\pm 1.04 \mathrm{Pa}$, which is far lesser than the SCX1DN error, being therefore neglected in the calculations.

2 PARAMETRIC DESIGN

A simple model based on the Poiseuille equation was created in a spreadsheet application to consider different gas properties (hydrogen and oxygen) and flow rate inlet conditions. From this analysis we concluded that increasing the number of parallel channels allows to handle greater flow rates and reduces the chances of channel blockage, but decreases the ability to accurately measure the pressure difference due to sensibility limitations of the sensor at low flow rates. A compromise solution was to use a 3 channels design. Three channel thicknesses of 0.1, 0.15 and 0.2 mm and 2 different channel lengths were selected for comparisons. The flow rates proposed were for 2 different conditions: the maximum flow capacity of the electrolyzer and the flow required by a PEMFC composed by a 10 cell stack and 12 A. Results for the first condition are shown on tables 1 and 2, while results for PEMFC operation are resumed on tables 3 and 4.

Table 1: Design parameters for electrolizer H_2 production, flowrate: 2 $[\mathrm{L/min}]$

Channels	h [mm]	w [mm]	L_{dp} [mm]	Δ P [Pa]	Sensor range [%]
3	0.1	20	50	3,333	48
	0.1	30	75	3,333	48
	0.15	6	50	3,292	48
	0.15	9	75	3,292	48
	0.2	3.75	50	3,333	48
	0.2	2.5	75	3,333	48

From these results, and in order to reach a design that can be machined without a high precision process, the final configuration will have a channel thickness of 0.1 mm. Also, in order to reach a design that will work for both scenarios, the final values of the parameters are

Table 2: Design parameters for electrolizer O_2 production, flowrate: 1 [L/min]

Channels	h [mm]	w [mm]	L_{dp} [mm]	Δ P [Pa]	Sensor range [%]
3	0.1	20	50	3,902	57
	0.1	30	75	3,902	57
	0.15	6	50	3,854	56
	0.15	9	75	3,854	56
	0.2	3.75	50	3,902	57
	0.2	2.5	75	3,902	57

Table 3: Design parameters for PEMFC H_2 consumption, flowrate: 0.54 [L/min]

Channels	h [mm]	w [mm]	L_{dp} [mm]	Δ P [Pa]	Sensor range [%]
3	0.1	5	50	3,627	53
	0.1	8	75	3,333	49
	0.15	1.5	50	3,582	52
	0.15	2.5	75	3,224	47
	0.2	0.65	50	3,487	51
	0.2	1	75	3,400	49

those shown in table 5, remarking the importance of the quality and sensitivity of the pressure transducer to obtain a multi-gas pressure difference flowmeter.

3 DESIGN VALIDATION AND OPTIMIZATION USING CFD

3.1 Mesh Domain

Both 2D and 3D CFD models of the final configuration were set up and simulated. To this end, structured two and three dimensional meshes were created on GMSH® Geuzaine and Remacle (2009).

3.2 Geometric configuration under study

As it is shown on Fig. 2, the model under study consists of inlet and outlet plena, 3 thin channels, and inlet and outlet measure static pressure ports, each one with its own additional plenum. Overall domain dimensions from the starting model are presented on table 6 as: inlet /

Table 4: Design parameters for PEMFC O_2 consumption, flowrate: 1.258 [L/min]

Channels	h [mm]	w [mm]	L_{dp} [mm]	Δ P [Pa]	Sensor range [%]
3	0.1	30	50	3,273	47
	0.1	40	75	3,682	53
	0.15	8	50	3,637	53
	0.15	12	75	3,637	53
	0.2	3.5	50	3,507	51
	0.2	5.5	75	3,348	49

Table 5: Flowmeter final design parameters

Origin	Channels	h [mm]	w [mm]	L_{dp} [mm]	Gas	flow rate [L/min]	Δ P [Pa]	Sensor range [%]
PEMFC	3	0.1	20	50	H_2	0.54	907	13
					O_2	1.26	4,910	71
Electrolizer					H_2	2	3,333	48
					O_2	1	3,902	57

outlet length (IL), inlet / outlet height (IH), channels span (CS), inlet / outlet plena length (PL), inlet / outlet height to first channel (CP), pressure port plena length (PPL) and pressure port diameter (PPD).

Table 6: Base design overall dimensions

Geometry	Dimension [mm]
IL	7.48
IH	11.3
CS	15
PL	5
CP	15
PPL	4
PPD	1

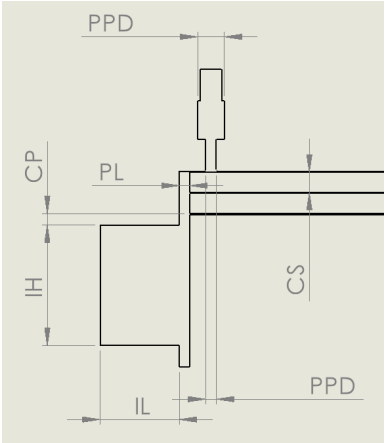

Figure 2: Flow meter prototype dimensions

On the following simulations, the geometric configuration is varied to study the effect of channel separation and plena sizes on the flow pattern. This will help us to decide a final global design, which in turn will impact directly on the selection of the most cost effective fabrication process fit for each component.

3.3 Grid independence test

The problem was solved using `simpleFoam`, as the flow is considered laminar and incompressible. The fluid selected was hydrogen and the inlet condition was a volumetric flow rate of 1.66e-6 m^3/s and a kinematic viscosity of 7.29e-5 m^2/s, corresponding to the electrolyzer production at 80 °C. Convergence criteria were set for residuals to 1e-5 for pressure and 1e-6 for velocity.

A grid independence test was carried out on 2 fully structured 2D meshes including increased refinement towards walls, to capture any wall effect. The pressure difference at the ports is compared with the analytical solution, as shown on table 7. They are values averaged over the hole axis of the pressure ports.

Table 7: Grid independence test

Mesh	Cells	$Pavg_{mid}$ [Pa]	Analytical [Pa]	diff [%]
M0-Coarse	8,173	3,229	3,333	3.12
M0-Regular	34,623	3,316	3,333	0.5
M0-Fine	70,553	3,335	3,333	0.07

3.4 CFD simulations

3.4.1 2D Study: Geometry optimization

For the spatial resolution parameter study, the regular mesh from the previous section was used. This exploratory approach was carried out with a 2D mesh because of the low computational time required to reach convergence plus the fact that the Poiseuille flow is essentially 2D except in a very narrow region in the front and back vertical walls of the channels.

The design refinement process consisted in starting with a proposed mesh (M0), with inlet and outlet connection ports of dimensions equivalent to those of the connection gas fittings, and channel length and width selected from Section 2. From this basic mesh, the domain was modified and the pressure difference at the pressure ports was checked in order to evaluate the impact of the geometry variation. If the numerical pressure difference is close enough to the analytical one, the geometry is deemed as acceptable, and the next geometry and mesh is built and simulated from previous one. The simulations were performed with the solver `simpleFoam`, under the same conditions of the grid independence test. Runs were carried out in a system Intel Core i7-4720HQ 2.60GHz, 16 Gb RAM.

The geometric variations were the following:

Table 8: 2D CFD Mesh description

Mesh	Description
M1-2D-H2	Reduced channel separation from 15 mm to 2 mm.
M2-2D-H2	Reduced inlet plenum length from 5 mm to 1 mm.
M3-2D-H2	Reduced outlet plenum length from 5 mm to 1 mm.
M4-2D-H2	Reduced distance from lower channel to gas connection from 15 mm to 1 mm.
M5-2D-H2	Reduced pressure port plenum length from 4 mm to 2.5 mm.

3.4.2 3D Study: Geometry verification

Once an optimized geometry was found, 3D simulations of a symmetrical configuration were carried out for hydrogen (M6). This was intended to detect possible flow behaviors that cannot be seen with 2 dimensional simulations. In order to reach a model related to a manufacturable version, a 3D mesh was developed from a new cad, where pressure ports are cylindrical objects. This resulted in a full hexahedral mesh of 1,174,000 cells. Simulations were run with `simpleFoam` with inlet flow rate of 1.66e-5 m^3/s and 8.33e-6 m^3/s for hydrogen and oxygen, respectively.

4 RESULTS

As shown on Table 9, the numerical pressure differences agree with the predicted analytical ones. On Table 10 values of pressure differences on the individual channels are reported. The small difference between the first and the other two channels is due to the collaboration of the dynamic pressure because of the deceleration of the flow inside the measuring port hole. This effect is less important when a 3D simulation is carried out. An example of the pressure gradient on the optimized geometry can be observed on Fig. 3.

A 3D effect was observed on the vicinity of the port hole connection to the channel, on both connectors, as is it shown on Fig. 4. This effect is due to the sudden expansion of the flow inside the connection hole. It affects the flow distribution along the width of the channel, being different in inlet and outlet, as can be seen on Fig. 5. In order to mitigate the impact of this phenomena, a new 3D simulation were carried out with a mesh where a 0.1 mm x $45°$ chamfer was added to the holes (M7), as it is shown on Fig. 6. This change in geometry reduced the swirl effect, more specifically in the outlet port, as is it reported on Fig. 7.

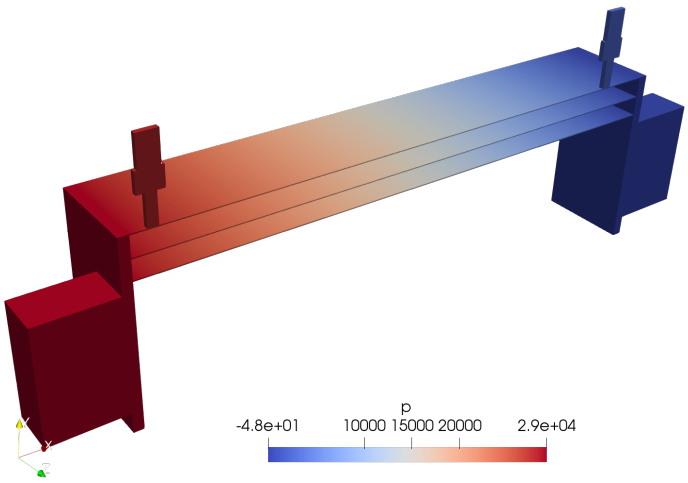

Figure 3: Hydrogen pressure drop simulation

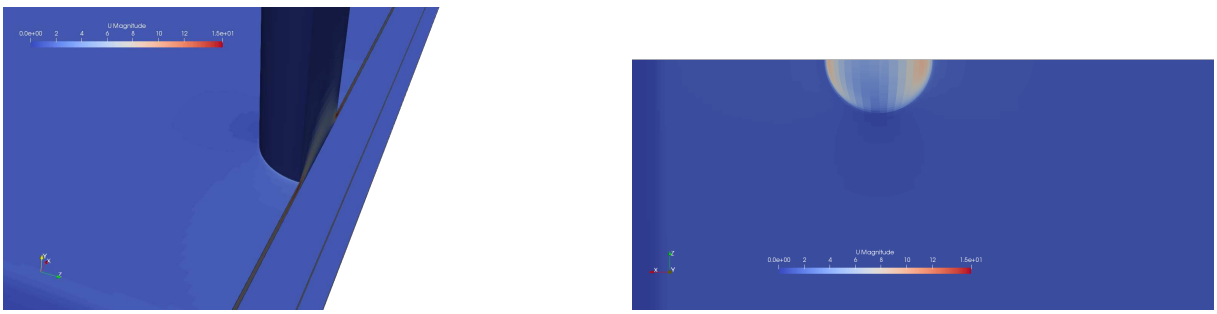

(a) Velocity contour view with pressure port

(b) Velocity contour effect

Figure 4: Velocity contour near inlet pressure port

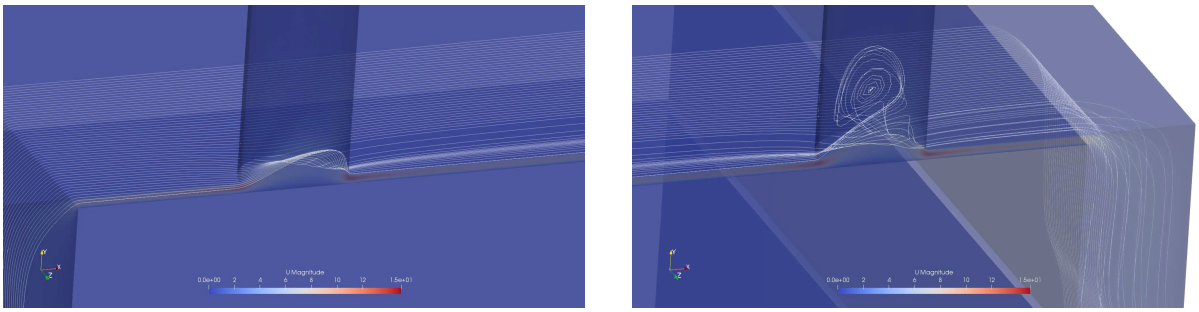

(a) Swirl inside pressure port near inlet (b) Swirl inside pressure port near outlet

Figure 5: Swirl effect around pressure measure holes

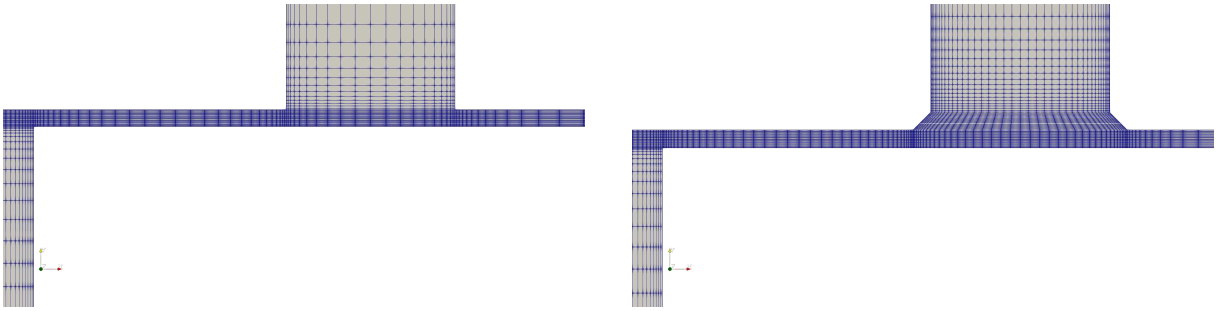

(a) Regular hole mesh (b) Hole mesh with chamfer

Figure 6: Pressure port geometry improve

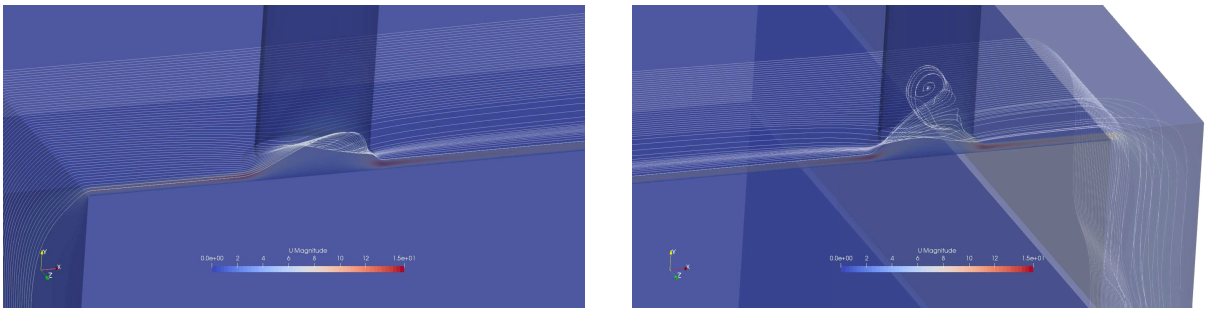

(a) Regular hole mesh (b) Hole mesh with chamfer

Figure 7: Pressure port geometry improvement

Table 9: CFD Geometry Verification Results

Mesh	Δ P [Pa]	diff-Analytical [%]
M1-2D-H2	3,316.02	0.52
M2-2D-H2	3,316.01	0.52
M3-2D-H2	3,315.80	0.53
M4-2D-H2	3,315.90	0.53
M5-2D-H2	3,315.84	0.52
M6-3D-H2	3,328.79	0.14
M7-3D-H2	3,329.13	0.13

Table 10: Channels pressure at position below inlet pressure port [Pa]

Mesh	channel 1	channel 2	channel 3	ch1 - ch2	ch1 - ch3
M1-2D-H2	1,967.99	1,965.06	1,965.05	2.93	2.90
M2-2D-H2	1,967.90	1,965.03	1,965.06	2.87	2.80
M3-2D-H2	1,967.60	1,968.65	1,968.45	2.95	3.10
M4-2D-H2	1,968.82	1,965.89	1,965.76	2.93	3.10
M5-2D-H2	1,968.77	1,965.85	1,965.72	2.92	3.00
M6-3D-H2	1,796.80	1,796.78	1,796.63	0.01	0.2
M7-3D-H2	1,795.39	1,795.37	1,795.22	0.01	0.2

5 CONCLUSIONS

OpenFOAM was applied as a fast and reliable tool to test models during the design process of an LFE flowmeter, helping to reduce production costs and reaching reliable designs.

As expected, channel geometry is paramount to the behavior of a Poiseuille mass flowmeter, so special attention must be paid to geometrical precision and surface tolerances. A lapping process is recommended in order to achieve a surface roughness below the 10 µm. Also, holes from pressure connection ports should be deburred and a chamfer added as possible to reduce the flow expansion effect inside them. Because this effect, other lFE based flowmeter designs measures the pressure difference on the inlet and outlet plena, adding the correction into the calculations for those areas where flow does not behave as Poiseuille.

A possible blockage of a channel means a higher flow rate in the rest of the set. Having a design where pressure difference is measured in only one channel makes it hard to determine if a variation of the pressure is due to a restriction of the channel or a change in the flowrate. This is the main reason why this kind of devices is restricted to dry and clean gases. For higher flowrates, where the LFE can be built with a greater number of channels, this event may be mitigated.

ACKNOWLEDGMENTS

The authors acknowledges to Dr. Giovanini (2021) for his support on the sensor selection, Mr. Francisco Nemiña for text formatting support and Techn. Santiago Gimenez from RINOX-S.A. (2021) and Eng. Pablo Vilar for theirs comments on the machining process.

REFERENCES

Baker R.C. *Flow Measurement Handbook: Industrial Designs, Operating Principles, Performance, and Applications*. Cambridge University Press, 2 edition, 2016. doi:10.1017/CBO9781107054141.

Controls F. https://www.gometrics.net/pdf/Catalogos-Furness/Furness-FCO96-brochure-ENG.pdf. 2021.

Geuzaine C. and Remacle J.F. Gmsh: a three-dimensional finite element mesh generator with built-in pre- and post-processing facilities. international journal for numerical methods in engineering. pages 1309–1331, 2009.

Giovanini L. http://sinc.unl.edu.ar/staff/leonardo-giovanini/. 2021.

Honeywell. https://sps.honeywell.com/us/en/products/sensing-and-iot/sensors/pressure-sensors/board-mount-pressure-sensors/scxl-series. 2021.

Meriam. https://www.meriam.com/assets/LFE-Brochure_1_15.pdf. 2021a.

Meriam. https://www.meriam.com/assets/LFE-User-Manual.pdf. 2021b.

OpenCFD. *OpenFOAM, The Open Source CFD Toolbox, User Guide*. OpenCFD Ltd., 2017.

Parmer C. https://www.coleparmer.com/c/differential-pressure-flowmeters". 2021.

RINOX-S.A. https://rinoxsa.com.ar/. 2021.